Estimation and attribution of water storage changes in regulated lakes based on Budyko's supply–demand framework

Mi Zhou
Wuhan University
Lihua Xiong (xionglh@whu.edu.cn)
Wuhan University
Gang Chen
Yunnan Survey and Design Institute of Water Conservancy and Hydropower
Jie Chen
Wuhan University
Dedi Liu
Wuhan University
Shuai Li
China Three Gorges Corporation

Research Article

Keywords: Lake water storage, Budyko framework, Regulated lake, Attribution analysis, Lake Dianchi

Posted Date: June 21st, 2022

DOI: https://doi.org/10.21203/rs.3.rs-1632974/v1

Abstract

Understanding changes in lake water storage (LWS) and its attribution to climate change and human activities is essential for adaptive management of water resources in regulated lakes. Although altimetric measurements, whether ground- or satellite-based, can reproduce LWS dynamics, they do not provide sufficient information on why LWS is changing. Neither the water balance method nor detailed hydrological modeling can capture exactly LWS change in most regulated lakes largely because of the scarcity of water output observations. Here, a simple water balance model, following Budyko's supply–demand framework, was proposed to estimate LWS change in regulated lakes without the need for water output information. The elasticity of LWS was theoretically derived from the Budyko-based model to attribute LWS change to its main driving factors. The annual LWS observed during 1964–2019 under three different regulation plans in Lake Dianchi, which is a typical regulated lake located in southwest China, was used to calibrate and test the proposed model. Comparison between the estimated results and observed data indicated that the model accurately captured the variations of annual LWS in Lake Dianchi with a relative root mean square error of 4.08%, and mean absolute percentage error of 2.88%. The attribution results suggested that lake regulation strategies were the primary cause of LWS change in Lake Dianchi, while water transfer had a limited contribution. This study suggests that complex hydrological behavior in regulated lakes can be explored using Budyko's supply–demand framework with a low requirement for data. This can provide effective guidance to lake managers and policymakers for adaptive management of water resources in regulated lakes.

1 Introduction

Lake water storage (LWS) is one of the most important geometric characteristics of natural lakes, and determines their ecological functions and socioeconomic values (Boehrer et al. 2010). Globally, LWS accounts for nearly three quarters of the readily accessible water resources on Earth (Molinos et al. 2015; Messager et al. 2016), and plays an essential role in ensuring water security and supporting water-related ecosystem services (Verpoorter et al. 2014; Mathis et al. 2016). However, LWS is highly sensitive to changes in regional environments because it incorporates the impacts of all natural and anthropogenic disturbances on the hydrological budget (Haghighi and Kløve 2015; Guo et al. 2015). Owing to the combined impacts of climate change and intensified human activities in recent decades, LWS is undergoing significant changes around the world, causing an increased risk to water security, degradation of lake-related ecosystems, and mismanagement of water resources (Gibson, et al. 2006a; Song et al. 2014; Pekel et al. 2016; Yang et al. 2016; Liu et al. 2019). Therefore, a better understanding of the response of LWS to natural and human-induced disturbances is extremely important for lake managers and policymakers.

In sparsely populated regions, LWS varies because of the imbalance between water inflows and outflows resulting from natural variability (Molinos et al. 2015). Therefore, long-term LWS change in near-natural lakes solely reflect the effect of climatic change occurring in the region (Song et al. 2014a). Several studies have been conducted to investigate the response of LWS to natural drivers such as precipitation, evapotranspiration and glacier shrinkage (Song et al. 2014b; Fan et al. 2021). Compared with that in sparsely populated regions, LWS in densely populated regions reflects the additional impacts from human activities, including water regulation. To better serve human needs, natural lakes in inhabited regions are mostly regulated by engineered control structures (e.g., levees, dams and sluices). Notable examples worldwide include Lake Ontario in America (Wilcox and Xie 2007), Lake Baikal in Asia (Jaguś et al. 2014), and Lake Victoria in Africa (Cetirana et al. 2020). Existing

studies show that the operation of engineered control structures has a significant effect on LWS dynamics by regulating lake outflows and dampening water level variability (Gibson et al. 2006b; Yin et al. 2013; Getirana et al. 2020). The water balance in regulated lakes is also subject to other human-induced disturbances (e.g., within-lake ecological restoration, inter-basin water transfer, irrigation and other withdrawals), which complicate the operational schemes for lake regulation and alter the variations in LWS (Veijalainen et al. 2010; Fergus et al. 2019; Getirana et al. 2020). The complicated hydrological behavior of regulated lakes brings challenges to understanding LWS dynamics and their response to the changing environment.

Although LWS changes can be estimated from the differences in the water level recorded at hydrometric stations (Yin et al. 2013; Xu et al. 2020) or monitored from satellite-based platforms (Zhang et al. 2006; Swenson and Wahr 2009; Han et al. 2020), these observational records alone may not provide sufficient information on why LWS is changing in regulated lakes (Lei et al. 2014). So far, previous efforts to address this issue were mostly made by means of water balance analysis, which derives LWS change as the difference between the water inputs and outputs of the lake (Chebud and Melesse 2009; Veijalainen et al. 2010; Hassan and Jin 2014; Zhang et al. 2019). As the closure term of the balance, an exact estimation of LWS change relies on accurate information on all the water input and output terms (Gronewold et al. 2020). However, these data are not available for most regulated lakes, especially for water output terms. Differ from these Newtonian methods with focusing on the physical processes in isolation, the Darwinian methods explain systematically the hydrological behavior as a whole, and propose an alternative way to capture the relevant processes through simple but effective empirical functions (Wang and Tang 2014). The most popular among these is Budyko hypothesis. Although the Budyko hypothesis was originally proposed to partition the annual water balance of natural, closed basins as a function of the ratio of available energy (the demand) to water (the supply) (Budyko 1958), recent efforts have generalized it as a supply–demand framework to partition available water into several components (Zhang et al. 2008; Wang, et al. 2011). Owing to its simplicity and ability to reflect complex hydrological processes with low data requirements, the generalized Budyko framework has been applied to explain various water-related processes, such as human water consumption (Lei et al. 2018), infiltration (Wang 2018), and baseflow (Cheng et al. 2020). Moreover, Budyko framework has been widely used to attribution analysis of hydrological components (e.g., runoff, soil water storage, and evapotranspiration) in response to climatic change and human activities (Wang and Hejazi 2011; Yang et al. 2020; Krajewski et al. 2021; Li et al. 2022). Similarly, there has been a potential need to develop such a Budyko-type model for assessing LWS changes in regulated lakes.

Actually, when the focus is on changes in LWS, it is not necessary to acquire detailed information on all output terms and these can be replaced by a total water output term. Hence, the available water in a lake can be partitioned into actual LWS and total water output. For regulated lakes, two operational water levels are typically specified in the regulation rules: maximum controllable and minimum drawdown (Parisopoulos et al. 2009). Therefore, apart from the constraint of the available water in the lake, actual LWS is also bounded by the effective storage capacity (i.e., the potential retention in the lake), which is controlled by the two water level limits for lake regulation. These two constraints on water balance in regulated lakes are similar to the water and energy constraints on catchment water balance (Budyko 1958). In a similar fashion to the Budyko-based estimation of evapotranspiration by partitioning precipitation without the need for streamflow information, there may be a potential alternative to LWS estimation through a Budyko-based partitioning of available water in regulated lakes without the need for water output information. Furthermore, the proposed Budyko model can be applied for sensitivity analysis to identify the main driving factors, and quantify their contribution to LWS change.

The objective of this study was (1) to propose a Budyko-based model that could estimate LWS change without prior information on water outputs; (2) to select a typical regulated lake to test the proposed model; and (3) to apply the elasticity method derived from the Budyko-based model to quantify the contribution of the main driving factors to LWS change. The reminder of this paper is organized as follows: the next section introduces the study area and data sources, Section 3 proposes the methods used in this paper, Section 4 presents the results and discussion, and the main conclusions are summarized in Section 5.

2 Study Area And Data Sources

2.1 Study area

The study site was the Lake Dianchi catchment with a total area of 2920 km^2, located in central Yunnan, southwest China (Fig. 1). The catchment is a semi-closed lake basin with only one natural outlet (the Haikou River) which drains into the Yangtze River. The catchment has a mountainous sub-tropical moist monsoon climate, with average annual temperature of 15.2°C, precipitation of 993 mm, and pan evaporation of 1211 mm. Almost one-tenth of the catchment is covered by Lake Dianchi, China's sixth-largest freshwater lake (Wang 1999), which has a surface area of 309 km^2. Located at the lowest point of the catchment, the lake receives water inflows from more than 30 centripetal rivers. The main inflowing tributaries are the Panlong River, Baoxiang River and Chai River.

<Fig. 1>

Although the area around the lake has been inhabited for approximately 2500 years by the ancestors of the Dian tribe, Lake Dianchi had a natural outflow in all historical periods until 1836 when the Lyfeng Sluice Gate was built at its outlet. Since then, the outflow of the lake has been regulated to facilitate the yearly dredging of the outflow river. In 1956, to mitigate the increasing conflict between flood control and water supply, the local government rebuilt the Lvfeng Gate and formulated an operational plan for lake regulation (hereafter referred to as Plan-1956). Under Plan-1956, the water level of Lake Dianchi was regulated within the range of 1887.2 m (upper limit) and 1885.5 m (lower limit). The inflow of excessive untreated sewage into the lake from accelerated population growth and increased demand for food production led to a rapid deterioration in water quality and severe eutrophication in 1980s (Liu et al. 2014). As a result, eco-environmental restoration became the primary objective of lake regulation, and local government enacted a revised regulation plan to incorporate the need for lake protection in 1988 (termed as Plan-1988). The upper limit of the water level was raised to 1987.4 m. Later in 1996, the lake was divided into two parts by an artificial dam with an added artificial outlet (Xiyuan Tunnel), which was built to increase the outflow capacity. In 2012, the regulation plan was further revised to optimize water quality improvement and the upper limit of the water level was raised to 1987.5 m (termed as Plan-2012). Furthermore, in 2013 the Niulanjiang-Dianchi Water Transfer Project (NDWTP) was built to transfer an annual mean 572 million m^3 of freshwater from outside the basin into Lake Dianchi to dilute the polluted water (Dai et al. 2016). Under these three different regulation plans, LWS estimated from water level records showed a significant increase during 1964–2019 (Fig. 2). For the adaptive management of water resources in the regulated lake, there is a pressing need to better understand the impacts of human activities such as lake regulation and inter-basin water transfer on LWS change.

2.2 Data sources

Long-term (1964–2019) monthly precipitation and other meteorological parameters (including precipitation, air temperature, wind speed, relative humidity, and sunshine duration) were collected from three meteorological stations, which are run by the Yunnan Meteorological Service (http://www.ynmb.cn). The water level records observed at two gauging stations, i.e., Haigeng (No. 17 in Fig. 1) and Haikou (No. 18 in Fig. 1), during 1964–2019 by the Yunnan Hydrological Bureau were used to represent the lake water levels. The water level–storage rating curve of Lake Dianchi was surveyed by the Kunming Bureau of Environmental Protection. Additionally, to simulate the lake inflow generated uniformly over the contributing basin, monthly precipitation data from 16 rain gauge stations within Lake Dianchi watershed were collected from Yunnan Hydrological Bureau. More detailed information about these stations can be found in Table 1.

Table 1
Hydro-meteorological data used in this study

Station No.	Station name	Altitude (m asl)	Type	Time span	Resolution	Source*
1	Ardalong	2180	Precipitation	1964–2019	monthly	YHB
2	Arziying	2100	Precipitation	1964–2019	monthly	YHB
3	Dashiba	2010	Precipitation	1964–2019	monthly	YHB
4	Zhonghe	2003	Precipitation	1964–2019	monthly	YHB
5	Songhuaba	1913	Precipitation	1964–2019	monthly	YHB
6	Huatingsi	2072	Precipitation	1964–2019	monthly	YHB
7	Sanjiacun	2200	Precipitation	1964–2019	monthly	YHB
8	Xibeishahe	1960	Precipitation	1964–2019	monthly	YHB
9	Dongbaishahe	1920	Precipitation	1964–2019	monthly	YHB
10	Dabanqiao	1965	Precipitation	1964–2019	monthly	YHB
11	Baoxianghe	2060	Precipitation	1964–2019	monthly	YHB
12	Hengchong	2003	Precipitation	1964–2019	monthly	YHB
13	Liangwangs	2810	Precipitation	1964–2019	monthly	YHB
14	Shuanglongwan	1923	Precipitation	1964–2019	monthly	YHB
15	Chaihe	1965	Precipitation	1964–2019	monthly	YHB
16	Shuanglong	1920	Precipitation	1964–2019	monthly	YHB
17	Haigeng	1888	Lake level	1964–2019	monthly	YHB
18	Haikou	1889	Lake level	1964–2019	monthly	YHB

Note: * YHB represents Yunnan Hydrological Bureau, YMS the Yunnan Meteorological Service.

Station No.	Station name	Altitude (m asl)	Type	Time span	Resolution	Source*
19	Chenggong	1907	Meteorological parameters	1964–2019	monthly	YMS
20	Jinning	1891	Meteorological parameters	1964–2019	monthly	YMS
21	Kunming	1891	Meteorological parameters	1964–2019	monthly	YMS
Note: * YHB represents Yunnan Hydrological Bureau, YMS the Yunnan Meteorological Service.						

3 Methods

The framework for this study is presented in Fig. 3. First, a Budyko-based lake water balance model was established to estimate LWS change in regulated lakes without the need for water output information. Second, the Shuffled Complex Evolution algorithm (SCE-UA) was used to calibrate model parameters. Third, the model performance and uncertainty of the simulatioactive LWS.n results were evaluated. Finally, quantitative attribution of LWS change was analyzed using the Budyko-based elasticity method.

3.1 Budyko-based LWS change estimation model

3.1.1 Lake water balance equation

The catchment of a lake can be conceptualized as a system of two regions: the lake surface and its contributing basin. The water balance of the lake can be written as (Haghighi and Kløve 2015)

$$S_l^{t-1} + \left(P_l^t - E_l^t\right)A_l^t + R_b^t A_b^t + I_c^t = S_l^t + O_r^t + O_g^t + O_h^t$$

1

where S_l is the LWS, P_l is the areal precipitation over the lake, E_l is the evaporation over the lake, R_b is the contributing basin runoff, A_b is the contributing area of the basin, A_l is the surface area of the lake, I_c is the channel inflow from outside the basin, O_r is the outflow through the lake-outlet rivers, O_g is the groundwater outflow, O_h is the human-induced water output associated with water diversion and withdrawal from the lake, and the superscripts t and (t-1) are used to denote the parameters in periods t and (t-1), respectively.

The most common strategy to estimate LWS change from the water balance relies on term-by-term estimation of the components comprising the above equation. On the left-hand side of Eq. (1), the areal precipitation over the lake P_l can be calculated from precipitation data gathered at the meteorological and/or rain gauge stations close to the lake using the Thiessen polygon method (Gibson et al. 2006b). Evaporation from the lake water surface E_l is estimated by the standard Penman-Monteith formulation (Allen et al. 1998). Basin runoff R_b is simulated by the dynamic water balance model (DWBM) (see subsection 3.1.4 for more details). Channel inflow from outside the basin I_c is usually measured. However, it is impossible to accurately estimate the three water output terms on

the right-hand side of Eq. (1) for most regulated lakes. For example, the outflow of regulated lakes can be estimated from the operation curve for regulation (Veijalainen et al. 2010; Han et al. 2021). However, actual outflow has been shown to deviate from the estimated results because lake regulation schemes needed to be corrected in real time (Lee et al. 1994; Parisopoulos et al. 2009). Therefore, the equation for estimating LWS change is not always closed.

3.1.2 Rearrangement of the lake water balance equation

For regulated lakes, there are two typical water levels in the regulation rules: maximum controllable h_{max} and minimum drawdown h_{min} (Parisopoulos et al. 2009). As illustrated in Fig. 4, h_{max} is set to the upper limit of the water level for flood prevention purpose, while h_{min} is commonly set to the lower limit of the water level for lake regulation without damage to the lake ecosystem (Veijalainen et al. 2010). Hence, of the water stored in the lake in period t, the portion above h_{min} is active (defined as active LWS), while the portion below h_{min} is static (static LWS). ThereforeEstimation of basin runoff, LWS may be determined by

$$S_l^t = S_{la}^t + S_{ls}^t$$

2

where S_{la} is the active LWS, and S_{ls} is the static LWS. To ensure sustainable use, water use should not exceed the active LWS.

Moreover, when focused on the change in LWS, detailedEstimation of basin runoff simulation of the three output terms is not necessary, and thus they can be replaced by a total water output term, such that

$$O_0^t = O_r^t + O_g^t + O_h^t$$

3

where O_0 is the total water output. For the case with a fixed h_{min}, the change in static LWS due to sedimentation can be negligible. Hence, substituting Eqs. (2) and (3) into Eq. (1), the lake water balance equation can be simplified as

$$S_{la}^{t-1} + \left(P_l^t - E_l^t\right)A_l^t + R_b^t A_b^t + I_c = S_{la}^t + O_0^t$$

4

From the perspective of water resources, this relationship indicates that water resources contained in the lake consist of the following three parts: naturally replenished, artificially replenished and stored (Izmailova 2018). The first part is water resources replenished through the natural water cycle, and includes tributary inflow, and precipitation minus evaporation from the lake, which is given by

$$W_n^t = \left(P_l^t - E_l^t\right)A_l^t + R_b^t A_b^t$$

5

in which W_n is the water resources replenished through the natural water cycle. The second part is water resources transferred from outside the basin through the inter-basin water transfer project, i.e.

$$W_a^t = I_c^t$$

6

in which W_a is the artificially replenished water resources. On the left-hand side of Eq. (4), the remaining term is the stored water resources, i.e.,

$$W_s^t = S_{la}^{t-1}$$

7

in which W_s is stored water resources. Therefore, the total usable water resources contained in the lake can be determined by

$$W_0^t = W_n^t + W_a^t + W_s^t$$

8

in which W_0 is the total usable water resources. Hence, substituting Eqs. (5)~(8) into Eq. (4), the lake water balance equation can be rewritten as

$$W_0^t = S_{la}^t + O_0^t$$

9

The relationship indicates that the total usable water resources in the lake is partitioned into active LWS and total water output. Similar to the Budyko hypothesis for estimating evapotranspiration through a simple partitioning of precipitation without the need for streamflow information, this study proposed a Budyko-based model to estimate active LWS by partitioning the total usable water resources in regulated lakes without the need for water output information.

3.1.3 Budyko-based model for LWS change estimation

The Budyko hypothesis was originally proposed to estimate the evapotranspiration ratio as a function of the ratio of available energy (the demand) to water (the supply) in natural, closed basins (Budyko 1958). More recently, it has been extended to solve various supply–demand balance problems in hydrological modeling on the basis of a supply–demand framework (Zhang et al. 2008; Lei et al. 2018; Simons et al. 2020). The general Fu-type expression for the extended Budyko framework is as follows (Zhang et al. 2008; Wang et al. 2011):

$$\frac{Z}{X} = F\left(\frac{Y}{X}, \alpha\right) = 1 + \frac{Y}{X} - \left[1 + \left(\frac{Y}{X}\right)^{\alpha}\right]^{1/\alpha}$$

10

in which F is the function symbol, X represents the supply, Y the demand, Z the consumption, and α is the consumption curve parameter with a range of (1, ∞).

To partition the total usable water resources in regulated lakes within Budyko's supply- demand framework, the "supply" term is the total usable water resources (X=W_0^t), and the "demand" term is the effective storage capacity, which is defined as the storage capacity between the two limits of the water level:

$$Y = S_e^t = S_{l*}^t - S_{ls}^t$$

11

in which S_e is the effective storage capacity of the lake, S_{l*} is the maximum LWS corresponding to the maximum controllable h_{max}, as shown in Fig. 4. Therefore, as the "consumption" term, the active LWS (Z=S_{la}^t) can be calculated as follows:

$$\frac{S_{la}^t}{W_0^t} = F\left(\frac{S_e^t}{W_0^t}, \alpha_1\right) = 1 + \frac{S_e^t}{W_0^t} - \left[1 + \left(\frac{S_e^t}{W_0^t}\right)^{\alpha_1}\right]^{1/\alpha_1}$$

12

in which α_1 is lake storage efficiency. The larger the value of α_1, the more water is stored in the lake, and the less is the water output from the lake. When $\alpha_1 \to \infty$, the term in Eq. (12) $\left[1 + \left(S_e^t / W_0^t\right)^{\alpha_1}\right]^{1/\alpha_1} \to 1$, then one has $S_{la}^t = S_e^t$. It indicates that the active LWS (the consumption) perfectly matches the effective storage capacity of the lake (the demand). In reality, the demand is often unmet, the active LWS is below both the effective storage capacity and the total usable water resources, as shown in Fig. 5. Then, the LWS change in period t can be estimated by

$$\Delta S_l^t = S_{la}^t - S_{la}^{t-1}$$

13

in which ΔS_l is the change in LWS.

3.1.4 Estimation of basin runoff

The DWBM proposed by Zhang et al. (2008) was applied to estimate basin runoff in this study. In the DWBM, the total precipitation over the basin P_b^t is partitioned into direct surface runoff R_d^t and catchment water retention Φ_b^t, which consists of soil storage change ΔS_b^t, basin evapotranspiration E_b^t, and ground water recharge R_g^t, as shown in Fig. 4. Considering the basin precipitation as the "supply" term in Eq. (10) (i.e., X=P_b^t), the potential basin water retention as the "demand" term (Y=Φ_{b*}^t), and the actual water retention over the basin as the "consumption" term (Z=Φ_b^t), the direct surface runoff is determined as follows:

$$R_b^t = P_b^t \left(1 - \frac{\Phi_b^t}{P_b^t}\right) = P_b^t \left[1 - F\left(\frac{\Phi_{b*}^t}{P_b^t}, \alpha_2\right)\right]$$

14

$$\Phi_{b*}^t = E_{b*}^t + S_{b*} - S_b^{t-1}$$

15

in which P_b is the basin precipitation, E_{b*} is the potential evapotranspiration of the basin, S_{b*} is the soil water storage capacity, S_b is the soil water storage. Φ_{b*} is the potential basin water retention, α_2 is the basin water retention efficiency. Then, in period t the total available water over the basin U_b^t, i.e., the sum of the basin water retention Φ_b^t and the residual soil storage in the previous period S_b^{t-1}, can be partitioned into the evapotranspiration opportunity Θ_b^t and groundwater recharge R_g^t. Considering the total available water over the basin as the "supply" term in Eq. (10) (i.e., $X = U_b^t$), the potential evapotranspiration opportunity as the "demand" term ($Y = \Theta_{b*}^t$), and actual evapotranspiration opportunity as the "consumption" term ($Z = \Theta_b^t$), the groundwater storage is determined by

$$G_b^t = (1 - k) G_b^{t-1} + U_b^t \left[1 - F\left(\frac{\Theta_{b*}^t}{U_b^t}, \alpha_3\right)\right]$$

16

$$\Theta_{b*}^t = E_{b*}^t + S_{b*}^t \,,\; U_b^t = \Phi_b^t + S_b^{t-1} \quad (17)$$

in which α_3 is the evapotranspiration efficiency, G_b is the groundwater storage, and k is the recession constant of groundwater. Treating groundwater storage as a linear reservoir, groundwater inflow into the lake is calculated as follows:

$$R_g^t = k \cdot G_b^{t-1}$$

18

in which R_g is groundwater inflow into the lake.

3.2 Parameter calibration and uncertainty analysis

The proposed model has five parameters, i.e., lake storage efficiency α_1 and four DWBM parameters (α_2, α_3, S_{b*}, and k), which need to be calibrated against measured data. The annual values of LWS were converted from the observed water level during the study period using the water level–storage rating curve. Then, the SCE-UA was applied to calibrate the parameters of the proposed model. (Duan et al. 1994). The performance of the proposed model was evaluated using two statistical indicators: relative root mean square error (RRMSE), and mean

absolute percentage error (MAPE). In the present study, four ratings of model performance were defined for RRMSE: excellent (RRMSE < 10%), good (10% ≤ RRMSE < 20%), common (20% ≤ RRMSE < 30%), and poor (RRMSE > 30%) (Zhou et al. 2020).

In addition, the 95% confidence limits of the total predicted uncertainties for LWS change were calculated using the Generalized Likelihood Uncertainty Estimation (GLUE) method (Beven and Binley 1992). Three summary statistics proposed by Xiong et al. (2009), namely the containing ratio, the average bandwidth, and the average deviation amplitude, were used to assess the uncertainty (Table 2).

Table 2
Statistical indicators used to evaluate the performance of the proposed model

Purpose	Statistical metrics	Equation	Perfect value
Model performance evaluation	Relative root mean square error (RRMSE)	$\mathrm{RRMSE} = \frac{1}{\mu_m}\sqrt{\frac{1}{T}\sum_{t=1}^{T}\left(v_m^t - v_e^t\right)^2}$	0
	Mean absolute percentage error (MAPE)	$\mathrm{MAPE} = \frac{1}{T}\sum_{t=1}^{T}\left\lvert\frac{v_e^t - v_m^t}{v_m^t}\right\rvert$	0
Uncertainty analysis	Containing Ratio (CR)	$\mathrm{CR} = \frac{N}{T}$	1
	Average Bandwidth (B)	$B = \frac{1}{T}\sum_{t=1}^{T}\left(v_{95\%\max}^t - v_{95\%\min}^t\right)$	0
	Average Deviation Amplitude (D)	$D = \frac{1}{T}\sum_{t=1}^{T}\left\lvert v_e^t - \frac{1}{2}\left(v_{95\%\max}^t + v_{95\%\min}^t\right)\right\rvert$	0

Note. v_m, v_e are measured and estimated values, respectively; μ_m is the average value of the measured data; $V_{95\%\max}^t$, $V_{95\%\min}^t$ represent the upper and lower bound values of the 95% confidence level, respectively; T is the length of data series, and N is the number of observed value that fall within the 95% confidence limits.

3.3 Attribution analysis of change in LWS

The elasticity method based on the Budyko framework was used to estimate the quantitative contribution of change in LWS in this study. First, starting with Eq. (2), the total differential of S_l can be expressed as

$$dS_l = \frac{\partial S_l}{\partial S_{la}} dS_{la} + \frac{\partial S_l}{\partial S_{ls}} dS_{ls}$$

19

The relative change in S_l can be expressed as follows:

$$\frac{dS_l}{S_l} = \frac{\partial S_l / S_l}{\partial S_{la} / S_{la}} \frac{dS_{la}}{S_{la}} + \frac{\partial S_l / S_l}{\partial S_{ls} / S_{ls}} \frac{dS_{ls}}{S_{ls}}$$

20

Similar to the definition of runoff elasticity (Roderick and Farquhar 2011), the elasticity of LWS to arbitrary independent variable x_1 can be calculated as

$$\eta_{x_1} = \frac{\partial S_l}{\partial x_1}\frac{x_1}{S_l} = \frac{x_1}{S_l}, x_1 = S_{la}, S_{ls} \quad (21)$$

in which η_x is the elasticity of S_l to the independent variable x_1. Hence, Eq. (20) can be rewritten as follows:

$$\frac{dS_l}{S_l} = \eta_{S_{la}}\frac{dS_{la}}{S_{la}} + \eta_{S_{ls}}\frac{dS_{ls}}{S_{ls}}$$

22

where $\eta_{S_{la}}$, $\eta_{S_{ls}}$ are the elasticities of LWS to active LWS and static LWS, respectively. As shown in Eq. (12), the change in active LWS are induced by changes in W_0, S_e and α_1, and the differential of S_{la} can be obtained by the following equations:

$$dS_{la} = \frac{\partial S_{la}}{\partial W_0}dW_0 + \frac{\partial S_{la}}{\partial S_e}dS_e + \frac{\partial S_{la}}{\partial \alpha_1}d\alpha_1$$

23

The relative change in S_{la} can be expressed as follows:

$$\frac{dS_{la}}{S_{la}} = \frac{\partial S_{la}/S_{la}}{\partial W_0/W_0}\frac{dW_0}{W_0} + \frac{\partial S_{la}/S_{la}}{\partial S_e/S_e}\frac{dS_e}{S_e} + \frac{\partial S_{la}/S_{la}}{\partial \alpha_1/\alpha_1}\frac{d\alpha_1}{\alpha_1}$$

24

Similarly, the elasticity of S_{la} to arbitrary independent variable x_2 can be calculated as

$$\varepsilon_{x_2} = \frac{\partial S_{la}}{\partial x_2}\frac{x_2}{S_{la}}, x_2 = W_0, S_e, \alpha_1 \quad (25)$$

in which ε_{x2} is the elasticity of S_{la} to the independent variable x_2. Then, Eq. (24) can be rewritten as follows:

$$\frac{dS_l}{S_l} = \varepsilon_{W_0}\frac{dW_0}{W_0} + \varepsilon_{S_e}\frac{dS_e}{S_e} + \varepsilon_{\alpha_1}\frac{d\alpha_1}{\alpha_1}$$

26

Setting $\varphi = S_e \Big/ W_0$, Eq. (12) becomes

$$\frac{S_{la}}{W_0} = f\left(\varphi, \alpha_1\right) = 1 + \varphi - \left(1 + \varphi^{\alpha_1}\right)^{\frac{1}{\alpha_1}}$$

27

where f is the function symbol. The elasticity coefficients of S_{ls} can be calculated as:

$\varepsilon_{W_0} = 1 - \frac{\varphi \cdot f_{\varphi}^{'}}{f\left(\varphi, \alpha_1\right)}$, {\varepsilon _{{S_e}}}=\frac{{\varphi \cdot f_{\varphi }^{'}}}{{f\left({\varphi ,{\alpha _1}} \right)}}, {\varepsilon _{{\alpha _1}}}=\frac{{{\alpha _1} \cdot f_{{{\alpha _1}}}^{'}}}{{f\left({\varphi ,{\alpha _1}} \right)}} (28)

Starting with Eq. (8), one has the differential of W_0 as follows:

d{W_0}=\frac{{\partial {W_0}}}{{\partial {W_n}}}d{W_n}+\frac{{\partial {W_0}}}{{\partial {W_a}}}d{W_a}+\frac{{\partial {W_0}}}{{\partial {W_s}}}d{W_s}
29

Defining the elasticities of W_0 to arbitrary independent variable x_3 as

{\xi _{{x_3}}}=\frac{{\partial {W_0}}}{{\partial {x_3}}}\frac{{{x_3}}}{{{W_0}}}=\frac{{{x_3}}}{{{W_0}}} , $x_3 = W_n, W_a, W_s$ (30)

The total differential of W_0 can be used to assess the change in the total usable water resources as follows:

\frac{{d{W_0}}}{{{W_0}}}={\xi _{{W_n}}}\frac{{d{W_n}}}{{{W_n}}}+{\xi _{{W_a}}}\frac{{d{W_a}}}{{{W_a}}}+{\xi _{{W_s}}}\frac{{d{W_s}}}{{{W_s}}}
31

Substituting Eqs. (26) and (31) into Eq. (22) yields

\frac{{d{S_l}}}{{{S_l}}}={\eta _{_{{{S_{ls}}}}}}\frac{{d{S_{ls}}}}{{{S_{ls}}}}+{\eta _{{W_n}}}\frac{{d{W_n}}}{{{W_n}}}+{\eta _{{W_a}}}\frac{{d{W_a}}}{{{W_a}}}+{\eta _{{W_s}}}\frac{{d{W_s}}}{{{W_s}}}+{\eta _{{S_e}}}\frac{{d{S_e}}}{{{S_e}}}+{\eta _{{\alpha _1}}}\frac{{d{\alpha _1}}}{{{\alpha _1}}}
32

in which the elasticities of S_l to W_n, W_a, W_s, S_e and α_1 are given by

{\eta _{{W_n}}}={\eta _{{S_{la}}}}{\varepsilon _{{W_0}}}{\xi _{{W_n}}}
33a
{\eta _{{W_a}}}={\eta _{{S_{la}}}}{\varepsilon _{{W_0}}}{\xi _{{W_a}}}
33b
{\eta _{{W_s}}}={\eta _{{S_{la}}}}{\varepsilon _{{W_0}}}{\xi _{{W_s}}}
33c
{\eta _{{S_e}}}={\eta _{{S_{la}}}}{\varepsilon _{{S_e}}}
33d
{\eta _{{\alpha _1}}}={\eta _{{S_{la}}}}{\varepsilon _{{\alpha _1}}}
33e

To reduce the influence of discretization error on LWS change attribution results, the average values of the elasticity coefficients in the pre-change (subscript *pre*) and post-change (subscript *post*) periods were used in practice (Jiang et al. 2015; Yang et al. 2020). Therefore, the relative contribution to change in LWS by arbitrary variable x_4 can be expressed as follows:

{\omega _{{x_4}}}=\frac{{\Delta S_{l}^{{{x_4}}}}}{{\Delta {S_l}}}=\frac{1}{2}\left({{\eta _{{S_{{x_4},pre}}}}+{\eta _{{S_{ls,post}}}} \right)\frac{{\Delta {x_4}}}{{{x_4}}}\frac{{{S_l}}}{{\Delta {S_l}}} \times 100\% , $x_4 = S_{ls}, W_n, W_a, W_s, S_e, \alpha_1$ (34)

in which {\omega _{{x_4}}} is the contribution of change in arbitrary variable x_4 ($x_4 = S_{ls}, W_n, W_a, W_s, S_e$ and α_1), ΔS_l is the change in LWS from the pre-change period to the post-change period, \Delta S_{l}^{{{x_4}}}is the change in LWS induced by arbitrary variable x_4, Δx_4 is the change in arbitrary variable x_4 from the pre-change period to the post-change period.

4 Results And Discussion

4.1 Estimation of LWS change in Lake Dianchi

4.1.1 Parameter calibration

Figure 2 shows that, for the upper water level limit, two breakpoints occurred, in 1988 and in 2012. Thus, the 56-year study period was split into three sub-periods, namely sub-period I under Plan-1956 (1964 to 1988), sub-period II under Plan-1988 (1989 to 2012), and sub-period III under Plan-2012 (2013 to 2019). Because different regulation plans were executed in the three sub- periods, parameter α_1 was calibrated for each sub-period. Previous studies have shown that, for a specific basin, the DWBM parameters ($\alpha_2, \alpha_3, S_{b*}$, and k) mainly depend on land use/cover (Xu et al. 2014; Gao et al. 2016). Because land use/cover change was more significant in the Lake Dianchi basin during recent decades owing to rapid urbanization which was characterized by an increase in constructed land and a decrease in grassland and cultivated land (Zhao et al. 2012; Wang et al. 2021), the four DWBM parameters were individually calibrated4.1.2 Model evaluation for the sub-periods involved in this study. To test the proposed model, the observed data in each sub- period were further divided into two groups: the first (approximately 70% of the data) was used for calibration, and the second was used for validation.

In the calibration procedure, when the proposed model matched the measured data reasonably well, the parameter α_1 was estimated as 1.64 for sub-period I, and the values of the DWBM parameters were $\alpha_2 = 4.55$, $\alpha_3 = 4.35$, S_{b*}=130 mm, and $k = 0.50$. A comparison of observed LWS with the estimated results from the proposed model, shown in Fig. 6, gave an RRMSE of 2.52%, and MAPE of 2.22%. For sub-period II, the values of model parameters for the fitted curve were $\alpha_1 = 2.22$, $\alpha_2 = 4.55$, $\alpha_3 = 3.57$, S_{b*}=100 mm, and $k = 0.45$, with a RRMSE of 5.47%, and MAPE of 3.97%. For sub-period III, the values of model parameters are $\alpha_1 = 2.63$, $\alpha_2 = 4.55$, $\alpha_3 = 3.57$, S_{b*}=100mm, and $k = 0.45$, with a RRMSE value of 2.17%, and MAPE value of 1.63%. For the study period as a whole, these resulted in an RRMSE of 4.08%, and MAPE of 2.88%.

The statistical indicators for model evaluation are shown in Table 3. The three studied sub-periods had RRMSE values of less than 10%, falling into the criteria of excellent performance. This indicated that the proposed model

was accurately calibrated for annual LWS change estimation in Lake Dianchi. Comparisons of estimated results with observed LWS in the three calibration periods are shown in Fig. 6.

Table 3
Performance metrics of annual LWS estimates from the proposed model

Period		MAPE (%)	RRMSE (%)	CR (%)	B (10^6 m^3)	D (10^6 m^3)
Sub-period I	Calibration	2.22	2.52	82	119	42
	Validation	4.00	5.07	38	86	76
Sub-period II	Calibration	3.97	5.47	38	116	75
	Validation	3.46	4.81	50	133	65
Sub-period III	Calibration	1.63	2.17	100	159	31
	Validation	1.18	1.42	100	172	14
Note: CR is the containing ratio, B is the average bandwidth, and D is the average deviation amplitude.						

4.1.2 Model evaluation

The validation sets were used to evaluate the performance of the calibrated model. Figure 6 shows comparisons of estimated and measured LWS for the three sub-periods with low RRMSEs, as listed in Table 3, which all meet the criteria of excellent performance. Table 3 also presents three uncertainty indicators for 95% confidence limits of total uncertainty for LWS during the three sub-periods. Overall, the results indicate that the proposed model has the ability to reasonably replicate LWS dynamics in Lake Dianchi.

4.2 Quantitative attribution of LWS change in Lake Dianchi

4.2.1 Changes in the supply term, demand term and parameter a_1

The proposed model with an annual time step was used to analyze attribution in this study. For convenience, the mean annual values of the arbitrary variable x_4 (x_4 = S_{ls}, W_n, W_a, W_s, S_e, and a_1) during the three sub-periods were denoted as x_{4}^{{\text{I}}}, x_{4}^{{{\text{II}}}}, and x_{4}^{{{\text{III}}}}, respectively. The change in the arbitrary variable x_4 was defined as

{\Delta _{{\text{I}} \to {\text{II}}}}\left({{x_4}} \right)=x_{4}^{{{\text{II}}}} - x_{4}^{{\text{I}}} , {\Delta _{{\text{II}} \to {\text{III}}}}\left({{x_4}} \right)=x_{4}^{{{\text{III}}}} - x_{4}^{{{\text{II}}}} (35)

in which {\Delta _{{\text{I}} \to {\text{II}}}}\left({{x_4}} \right) is the change of x_4 from sub-period I to sub-period II, and {\Delta _{{\text{I}} \to {\text{II}}}}\left({{x_4}} \right) is the change of x_4 from sub-period II to sub-period III.

As shown in Table 4, in sub-period I $W_{0,I}$ was equal to 776 million m^3, of which approximately 62% was attributed to W_{n}^{{\text{I}}} through the natural hydrological cycle. In sub-period II, W_{0}^{{{\text{II}}}} increased to 966 million m^3 (i.e., {\Delta _{{\text{I}} \to {\text{II}}}}\left({{W_0}} \right)=190 million m^3). Because the stored water resources increased by 145 million m^3, the portion of W_{n}^{{{\text{II}}}} decreased to 54%. In sub-period III, because channel inflow of 397 million m^3 was transferred into the lake through the NDWTP, the total usable water increased to 1506 million m^3 (i.e., {\Delta _{{\text{II}} \to {\text{III}}}}\left({{W_0}} \right)= 54 million m^3), and the proportion of W_{n}^{{{\text{III}}}} sharply decreased to 39%. These results demonstrate that the composition of the total usable water resources in Lake Dianchi changed from being mainly dependent on the natural hydrological cycle in sub-periods I and II to being controlled by human activities in sub-period III. Meanwhile, owing to the increase in the maximum controllable level, the effective storage capacity increased from 510 million m^3 in sub-period I to 571 million m^3 in sub-period II, which indicates a S_e increase of 61 million m^3 in sub-period II relative to sub-period I. Similarly, a S_e increase of 31 million m^3 occurred in sub-period III relative to sub-period II. The values of parameter α_1 for the three sub-periods were 1.64, 2.22 and 2.63, which indicated a {\Delta _{{\text{I}} \to {\text{II}}}}\left({{\alpha _1}} \right) value of 0.58 and a {\Delta _{{\text{II}} \to {\text{III}}}}\left({{\alpha _1}} \right) value of 0.41.

Table 4
Mean and relative changes of main factors attributable to LWS changes in Lake Dianchi

Sub-period	Supply						Demand		Parameter	
	W_n (10^6 m^3)		W_a (10^6 m^3)		W_s (10^6 m^3)		S_e (10^6 m^3)		α_1	
	Mean	Change	Average	Change	Mean	Change	Mean	Change	Mean	Change
I	478	–	0	–	298	–	510	–	1.64	–
II	523	45	0	0	442	144	571	61	2.22	0.58
III	579	56	397	397	519	77	602	31	2.63	0.41

4.2.2 Quantitative attribution of LWS change

Overall, elasticity coefficients of LWS were positively correlated with W_n, W_a, W_s, S_{ls}, S_e and parameter α_1 during the three sub-periods (Table 5). The values were largest for S_{ls}, intermediate for S_e and α_1, and smallest for W_a. Over time, the value of η_{Se} increased during the three sub-periods but both η_{Wn} and $\eta_{\alpha 1}$ decreased, which suggests that LWS became more sensitive to the lake water level regulations but less sensitive to climate change and lake storage efficiency. In sub-period III with the inter-basin water transfer through the NDWTP, the value of η_{Wa} was 0.02, indicating that a 10% increase in channel inflow from outside the basin would increase LWS by 0.2%.

Table 5
Quantitative contributions of LWS change in Lake Dianchi

Sub-period	Elasticity of LWS						Quantitative contribution to LWS change (%)					
	η_{Sls}	η_{Wn}	η_{Wa}	η_{Ws}	η_{Se}	$\eta_{\alpha 1}$	ω_{Sls}	ω_{Wn}	ω_{Wa}	ω_{Ws}	ω_{Se}	$\omega_{\alpha 1}$
I	0.77	0.06	0	0.04	0.13	0.31	–	–	–	–	–	–
II	0.69	0.07	0	0.06	0.19	0.20	0.0	5.3	0.0	14.9	15.9	63.7
III	0.64	0.02	0.01	0.02	0.30	0.12	0.0	7.8	12.9	10.2	23.2	45.9
Average	0.70	0.05	0.01	0.04	0.20	0.21	0.0	6.6	6.5	12.6	19.6	54.9

The relative contributions of variations in W_n, W_a, W_s, S_{ls}, S_e and parameter α_1 are also shown in Table 5. The main factors influencing the change in LWS varied in the different sub-periods. The increased LWS in sub-period II was controlled by changes in lake storage efficiency (up to 63.7%), whereas the change in W_n had a minor impact on LWS increase. For sub-period III, the contribution of changes in W_a and S_e to the increased LWS was 12.9% and 23.2%, respectively (Table 5), whereas the contribution of changes in W_n further reduced to 7.8%. Notably, the changes in W_a and S_e owing to the alteration of lake regulation strategies became more pronounced.

4.3 Controls of LWS dynamics in regulated Lake Dianchi

Figure 7 depicts the scatter plots of the actual storage ratio S_{la}/W_0 against S_e/W_0 in Lake Dianchi during the three sub-periods. Similar to the observed behavior in the original Budyko curves, as S_e/W_0 increased, S_{la}/W_0 increased within the two limits. Clearly, the effect of lake storage efficiency α_1 on S_{la}/W_0 was minimal under the two extreme conditions. This was because under these conditions, LWS was dominated by W_0 and S_e, respectively. When S_e/W_0 was approximately 1, the actual storage ratio S_{la}/W_0 showed maximum sensitivity to α_1. One possible explanation is that in this condition, both W_0 and S_e had the same control over active LWS change, and thus the lake regulation rules imposed a larger impact on LWS change. The results indicate that the LWS dynamics in this studied lake are subject to the supply and demand of the lake water circulation system. Most of the data points fall within the water-storage-limited zone, i.e., $S_e/W_0 < 1$, as shown in Fig. 7, which indicates that Lake Dianchi is an apparent water-storage-limited lake.

<Fig. 7>

It should be noted that during each sub-period under the same regulation scheme, the α_1 value can be fixed as a constant, which enables the model to predict further LWS change in regulated lakes. According to a literature survey, the Lvfeng Gate at the outlet river has an insufficient discharge capacity. To minimize the flood risk, the regulators limited the water level of Lake Dianchi during sub-period I below 1886.7 m, which was lower than the assigned value of 1887.2 m in Plan-1964. If the actual upper limit of water level was used for calculation, the effective storage capacity S_e in sub-period I was reduced to 358 million m^3. As a result, the calibrated value of α_1 increased to 2.00 for the best fitted curve. This indicates that the value of α_1 is closely related to S_e. The smaller the S_e value, the larger the α_1 value.

4.4 Comparison with the water balance method

On the basis of the reservoir routing model proposed by Hanasaki et al. (2006) (thereafter referred to as HM), the water balance method was used to assess the relative performance of the proposed model. The non-irrigation HM was selected to estimate outflow, which is expressed as (Hanasaki et al. 2006):

Q_{0}^{t}=\left\{ \begin{gathered} \frac{1}{C}\frac{{S_{l}^{t - 1}}}{{S_{l*}}}Q_{{in}}^{t}, {\text{IR}} \geqslant 0.5 \hfill \\ \frac{1}{C}\frac{{S_{l}^{t - 1}}}{{S_{l*}}}{\left({\frac{{{\text{IR}}}}{{0.5}}} \right)^2}Q_{{in}}^{t}+\left[{1 - {{\left({\frac{{{\text{IR}}}}{{0.5}}} \right)}^2}} \right]Q_{{in}}^{t}{\text{,}} {\text{IR}}<0.5 \hfill \\ \end{gathered} \right. 36

in which {\text{IR}}\left({={{{S_{l*}}} \mathord{\left/ {\vphantom {{{S_{l*}}} {{I_0}}} \right. \kern-0pt} {{I_0}}} \right) is the impoundment ratio of the lake, where I_0 is the mean annual inflow (m^3/yr); Q_{in} is the inflow; and C is a dimensionless coefficient, which was fixed at 0.85 by Hanasaki et al. (2006). In the present study, the value of C was calibrated within the range of 0.1 to 1.5.

The annual LWS estimated by the proposed model and the HM-based water balance method is plotted in Fig. 8. It can be seen that the proposed model matches quite well with the observed LWS dynamics, while HM-based water balance method is likely to underestimate LWS, especially in dry years (e.g., 2009–2013). The proposed model has a lower RRMSE of 4.08% than that of HM-based water balance method of 16.37%. These results occurred most likely because HM ignores the impact of the minimum drawdown level on outflow, which may produce a large error in outflow, and eventually in the closure term of the water balance (i.e., LWS change). By comparison, the proposed model not only incorporates the impacts of both total usable water resources and water level control within Budyko's demand-supply framework, but also eliminates the outflow error from the estimated LWS change. Thus, it may be a better candidate for estimating LWS change in regulated lakes.

4.5 Implications of the proposed model

Adaptive management of water resources in regulated lakes is the key challenge for lake managers and policymakers. The present study provides a simple method for estimating the variation of LWS in regulated lakes from the perspective of the water supply and demand balance. On this basis, the elasticity method can be applied to separate the impacts of the main controlling factors such as lake regulation activities and inter-basin water transfer on LWS change in regulated lakes. Owing to its simplicity and low data requirements, this method can be feasibly implemented to determine low-cost but effective water resources management strategies. This model can be applicable for regulated lakes to predict future LWS under the specified regulation scheme, reconstruct outflow time series, and assess the influence of inter-basin water transfer on lake level fluctuations.

5 Conclusions

Following Budyko's supply–demand framework, this study proposed a water balance model to estimate annual LWS change without the need for water output information. The study found that the proportion of active LWS was controlled by the total usable water resources and the effective storage capacity of the lake. The impacts of the main driving factors on LWS were investigated using the elasticity method. The proposed model was applied to Lake Dianchi, a typical regulated lake located in southwest China. The main conclusions derived from the present study are as follows.

(1) Plotting the actual storage ratio S_{la}/W_0 against the potential storage ratio S_e/W_0 in Lake Dianchi showed a Budyko-type relationship, exhibiting a monotonically increasing shape within two limits. The results revealed that total usable water resources and effective storage capacity controlled the variability of LWS change in the regulated lake.

(2) The proposed model was capable of estimating LWS change in a regulated lake with reasonable accuracy. Compared with the HM-based water balance method, the model was more effective at capturing LWS dynamics in Lake Dianchi because it accounted for the effects of total usable water resources, water level control and lake regulation with the estimation error of outflow eliminated in the water balance.

(3) The lake regulation strategy was the most important factor affecting the change in LWS in Lake Dianchi, contributing to an increase of 54.9% in LWS on average, while the inter-basin water transfer made a relatively limited contribution in determining LWS change. This is especially useful for adaptive management of water resources in the regulated lake.

Declarations

Author Contributions M Zhou: Conceptualization, Methodology, Software, Formal analysis, Writing - Original Draft. L Xiong: Conceptualization, Resources, Writing - Review & Editing, Project administration, Funding acquisition. G Chen: Data collection, Writing-Review & Editing. J Chen: Resources, Writing - Review & Editing. DD Liu: Writing - Review & Editing. S Li: Software, Writing - Review & Editing. All authors read and approved the final manuscript.

Funding This research was financially supported by National Natural Science Foundation of China (NSFC Grants 41890822 and 51525902), the National Key R&D Program of China (2017YFC0405901), and the Ministry of Education “Plan 111” Fund of China (B18037), all of which are greatly appreciated.

Availability of Data All data are available from the corresponding author upon reasonable request.

Ethical Approval The author promises to compliance with Ethical Standards.

Consent to Participate Informed consent was obtained from all individual participants included in the study.

Consent to Publish The participants have consented to the submission of the research article to the journal.

Competing Interests The authors declare they have no conflict of interest.

References

1. Allen RG, Pereira LS, Raes D, Smith M (1998) Crop Evapotranspiration: Guidelines for Computing Crop Requirements. FAO Irrigation and Drainage Paper No. 56, Rome, Italy, p. 300
2. Beven K, Binley A (1992) The future of distributed models-model calibration and uncertainty prediction. Hydrol Process 6(3):279–298
3. Boehrer B, Kastner S, Ollesch G (2010) High accuracy measurements of water storage change in Mining Lake 111. Ger Limnol 40:156–160

4. Budyko MI (1958) The Heat Balance of the Earth's Surface. US Department of Commerce, Washington, DC
5. Chebud A, Melesse M (2009) Modelling lake stage and water balance of Lake Tana, Ethiopia. Hydrol Process 23:3534–3544
6. Chen H, Huo Z, Zhang L, White I (2020) New perspective about application of extended Budyko formula in arid irrigation district with shallow groundwater. J Hydrol 582:124496
7. Cheng S, Cheng L, Liu P, Qin S, Zhang L, Xu CY, Xiong L, Liu L, Xia J (2021) An Analytical Baseflow Coefficient Curve for Depicting the Spatial Variability of Mean Annual Catchment Baseflow. Water Resour Res 57:e2020WR029529
8. Dai C, Tan Q, Lu WT, Liu Y, Guo HC (2016) Identification of optimal water transfer schemes for restoration of a eutrophic lake: an integrated simulation-optimization method. Ecol Eng 95:409–421
9. Duan Q, Sorooshian S, Gupta VK (1994) Optimal use of the SCE-UA global optimization method for calibrating watershed models. J Hydrol 158:265–284
10. Fan C, Song C, Liu K, Ke L, Xue B, Chen T, Fu C, Cheng J (2021) Century-scale reconstruction of water storage changes of the largest lake in the Inner Mongolia Plateau Using a machine learning approach. Water Resour Res 57:e2020WR028831
11. Fergus CE, Brooks JR, Kaufmann PR, Herlihy AT, Pollard AI, Weber MH, Paulsen SG (2019) Lake water levels and associated hydrologic characteristics in the conterminous U.S. J Am Water Resour Assoc 56(3):1–22
12. Getirana A, Jung HC, Hoek JVD, Ndehedehe CE (2020) Hydropower dam operation strongly controls Lake Victoria's freshwater storage variability. Sci Total Environ 726:138343
13. Gibson JJ, Prowse TD, Peters DL (2006a) Partitioning impacts of climate and regulation on water level variability in Great Slave Lake. J Hydrol 329:196–206
14. Gibson JJ, Prowse TD, Peters DL (2006b) Hydroclimatic controls on water balance and water level variability in Great Slave Lake. Hydrol Process 20:4155–4172
15. Gronewold AD, Smith JP, Read LK, Crooks JL (2020) Reconciling the water balance of large lake systems. Adv Water Res 137:103505
16. Guo M, Wu W, Zhou XD, Chen YM, Li J (2015) Investigation of the dramatic changes in lake level of the Bosten Lake in northwestern China. Theor Appl Climatol 119:341–351
17. Haghighi AT, Kløve B (2015) A sensitivity analysis of lake water level response to changes in climate and river regimes. Limnologica 51:118–130
18. Han Z, Long D, Huang Q, Li X, Zhao F, Wang J (2020) Improving reservoir outflow estimation for ungauged basins using satellite observations and a hydrological model. Water Resour Res 56:e2020WR027590
19. Hanasaki N, Kanae S, Oki T (2006) A reservoir operation scheme for global river routing models. J Hydrol 327:22–41
20. Hassan AA, Jin S (2014) Lake level change and total water discharge in East Africa Rift Valley from satellite-based observations. Glob Planet Change 117:79–90
21. Izmailova AV (2018) Lake water resources in the Asian Part of the Russian Federation. Water Resour 45(5):633–641
22. Jaguś A, Rzętała MA, Rzętała M (2015) Water storage possibilities in Lake Baikal and in reservoirs impounded by the dams of Angara River cascade. Environ Earth Sci 73:621–628

23. Jiang C, Xiong L, Wang D, Liu P, Guo S, Xu CY (2015) Separating the impacts of climate change and human activities on runoff using the Budyko-type equations with time-varying parameters. J Hydrol 522:326–338
24. Krajewski A, Sikorska-Senoner AE, Hejduk L, Banasik K (2021) An attempt to decompose the impact of land use and climate change on annual runoff in a small agricultural catchment. Water Resour Manage 35:881–896
25. Lee DH, Quinn FH, Sparks D, Rassam JC (1994) Modification of Great Lakes regulation plans for simulation of maximum Lake Ontario outflows. J Great Lakes Res 20(3):569–582
26. Li S, ·Du T, Gippel CJ (2018) A modified Fu (1981) equation with a time–varying parameter that improves estimates of inter–annual variability in catchment water balance. Water Resour Manage 36:1645–1659
27. Lei X, Zhao J, Wang D, Sivapalan M (2018) A Budyko-type model for human water consumption. J Hydrol 567:212–226
28. Lei Y, Yang K, Wang B, Sheng Y, Bird BW, Zhang G, Tian L (2014) Response of inland lake dynamics over the Tibetan Plateau to climate change. Clim Change 125:281–290
29. Liu H, Chen Y, Ye Z, Li Y, Zhang Q (2019) Recent Lake Area changes in central Asia. Sci Rep 9:16277
30. Liu Y, Wang YL, Sheng H, Dong FF, Zou R, Zhao L, Guo HC, Zhu X, He B (2014) Quantitative evaluation of lake eutrophication responses under alternative water diversion scenarios: A water quality modeling based statistical analysis approach. Sci Total Environ 468–469:219–227
31. Molinos JG, Viana M, Brennan M, Donohue I (2015) Importance of long-term cycles for predicting water level dynamics in natural lakes. PLoS ONE 10(3):e0119253
32. Messager ML, Lehner B, Grill G, Nedeva I, Schmitt O (2016) Estimating the volume and age of water stored in global lakes using a geo-statistical approach. Nat Comm 7:13603
33. Parisopoulos GA, Malakou M, Giamouri M (2009) Evaluation of lake level control using objective indicators: The case of Micro Prespa. J Hydrol 367:86–92
34. Pekel JF, Cottam A, Gorelick N, Belward AS (2016) High-resolution mapping of global surface water and its long-term changes. Nature 540:418–422
35. Roderick ML, Farquhar GD (2011) A simple framework for relating variations in runoff to variations in climatic conditions and catchment properties. Water Resour Res 47:W00G07
36. Simons GWH, Bastiaanssen WGM, Cheema MJM, Ahmad B, Immerzeel WW (2020) A novel method to quantify consumed fractions and non-consumptive use of irrigation water: application to the Indus basin irrigation system of Pakistan. Agric Water Manag 236:106174
37. Song C, Huang B, Ke L (2014a) Inter-annual changes of alpine inland lake water storage on the Tibetan Plateau: Detection and analysis by integrating satellite altimetry and optical imagery. Hydrol Process 28:2411–2418
38. Song C, Huang B, Richards K, Ke L, Hien PV (2014b) Accelerated lake expansion on the Tibetan Plateau in the 2000s: induced by glacial melting or other processes? Water Resour Res 50:3170–3186
39. Swenson S, Wahr J (2009) Monitoring the water balance of Lake Victoria, East Africa, from space. J Hydrol 370:163–176
40. Veijalainen N, Dubrovin T, Marttunen M, Vehviläinen B (2010) Climate change impacts on water resources and lake regulation in the Vuoksi watershed in Finland. Water Resour Manage 24:3437–3459

41. Verpoorter C, Kutser T, Seekell DA, Tranvik LJ (2014) A global inventory of lakes based on high-resolution satellite imagery. Geophys Res Lett 41:6396–6402
42. Wang S (1999) China Lakes Chronicle. Science Press Nanjing
43. Wang D (2018) A new probability density function for spatial distribution of soil water storage capacity leads to the SCS curve number method. Hydrol Earth Syst Sci 22:6567–6578
44. Wang D, Hejazi M (2011) Quantifying the relative contribution of the climate and direct human impacts on mean annual streamflow in the contiguous United States. Water Resour Res 47: W00J12
45. Wang D, Tang Y (2014) A one-parameter Budyko model for water balance captures emergent behavior in Darwinian hydrologic models. Water Resour Res 47:4569–4577
46. Wang QJ, Pagano TC, Zhou SL, Hapuarachchi HAP, Zhang L, Robertson DE (2011) Monthly versus daily water balance models in simulating monthly runoff. J Hydrol 404:166–175
47. Wang R, Xu X, Bai Y, Alatalo JM, Yang Z, Yang W, Yang Z (2014) Impacts of Urban Land Use Changes on Ecosystem Services in Dianchi Lake Basin, China Sustainability 2021, 13: 4813
48. Wilcox DA, Xie Y (2007) Predicting wetland plant community responses to proposed water level regulation plans for Lake Ontario: GIS-based modeling. J Great Lakes Res 33:751–773
49. Xiong L, Wan M, Wei X, O'Connor KM (2009) Indices for assessing the prediction bounds of hydrological models and application by generalized likelihood uncertainty estimation. Hydrol Sci J 54(5):852–871
50. Xu Y, Li J, Wang J, Chen J, Liu Y, Ni S, Zhang Z, Ke C (2020) Assessing water storage changes of Lake Poyang from multi-mission satellite data and hydrological models. J Hydrol 590:125229
51. Yang H, Xiong L, Xiong B, Zhang Q, Xu CY (2020) Separating runoff change by the improved Budyko complementary relationship considering effects of both climate change and human activities on basin characteristics. J Hydrol 591:125330
52. Yin Y, Chen Y, Yu S, Xu W, Wang W, Xu Y (2013) Maximum water level of Hongze Lake and its relationship with natural changes and human activities from 1736 to 2005. Quat Int 304:85–94
53. Zhang J, Xu K, Yang Y, Qi L, Hayashi S, Watanabe M (2006) Measuring water storage fluctuations in Lake Dongting, China, by Topex/Poseidon satellite altimetry. Environ Monit Assess 115:23–37
54. Zhang M, Wang S, Gao G, Fu B, Ye Z, Shen Q (2019) Exploring responses of lake area to river regulation and implications for lake restoration in arid regions. Ecol Eng 94:629–637
55. Zhang L, Potter N, Hickel K, Zhang Y, Shao Q (2008) Water balance modeling over variable time scales based on the Budyko framework: model development and testing. J Hydrol 360:117–131
56. Zhao Y, Zhang K, Fu Y, Zhang H (2012) Examining land-use/land-cover change in the Lake Dianchi watershed of the Yunnan-Guizhou plateau of southwest China with remote sensing and GIS techniques: 1974–2008. Int J Environ Res Public Health 9:3843–3865
57. Zhou M, Chen G, Dong Z, Xie B, Gu S, Shi P (2020) Estimation of surface albedo from meteorological observations across China. Agric For Meteor 281:107848

Figures

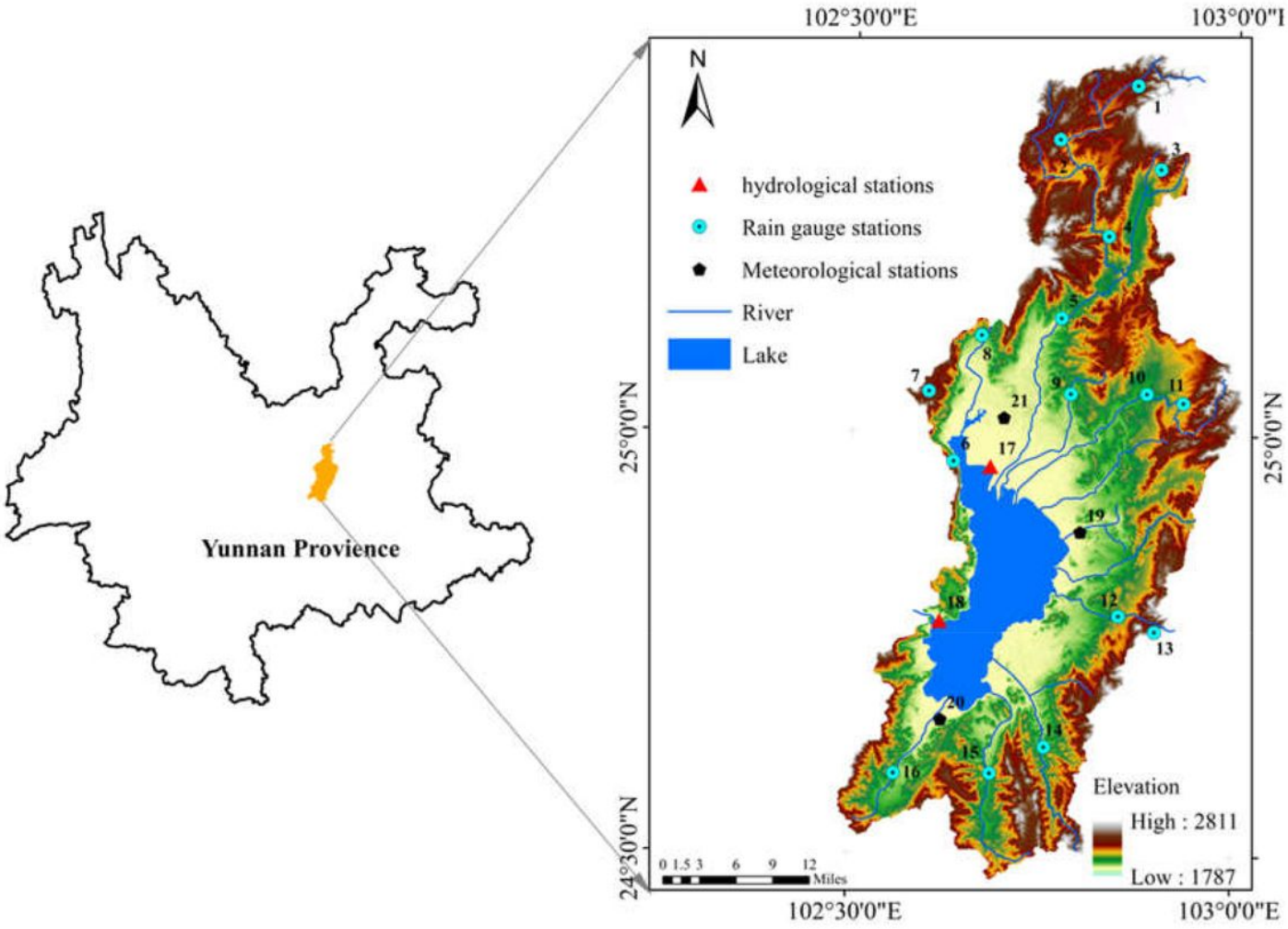

Figure 1

Geographical location, topography, lake, river networks, rain gauge stations, hydrological stations and meteorological stations in Lake Dianchi catchment

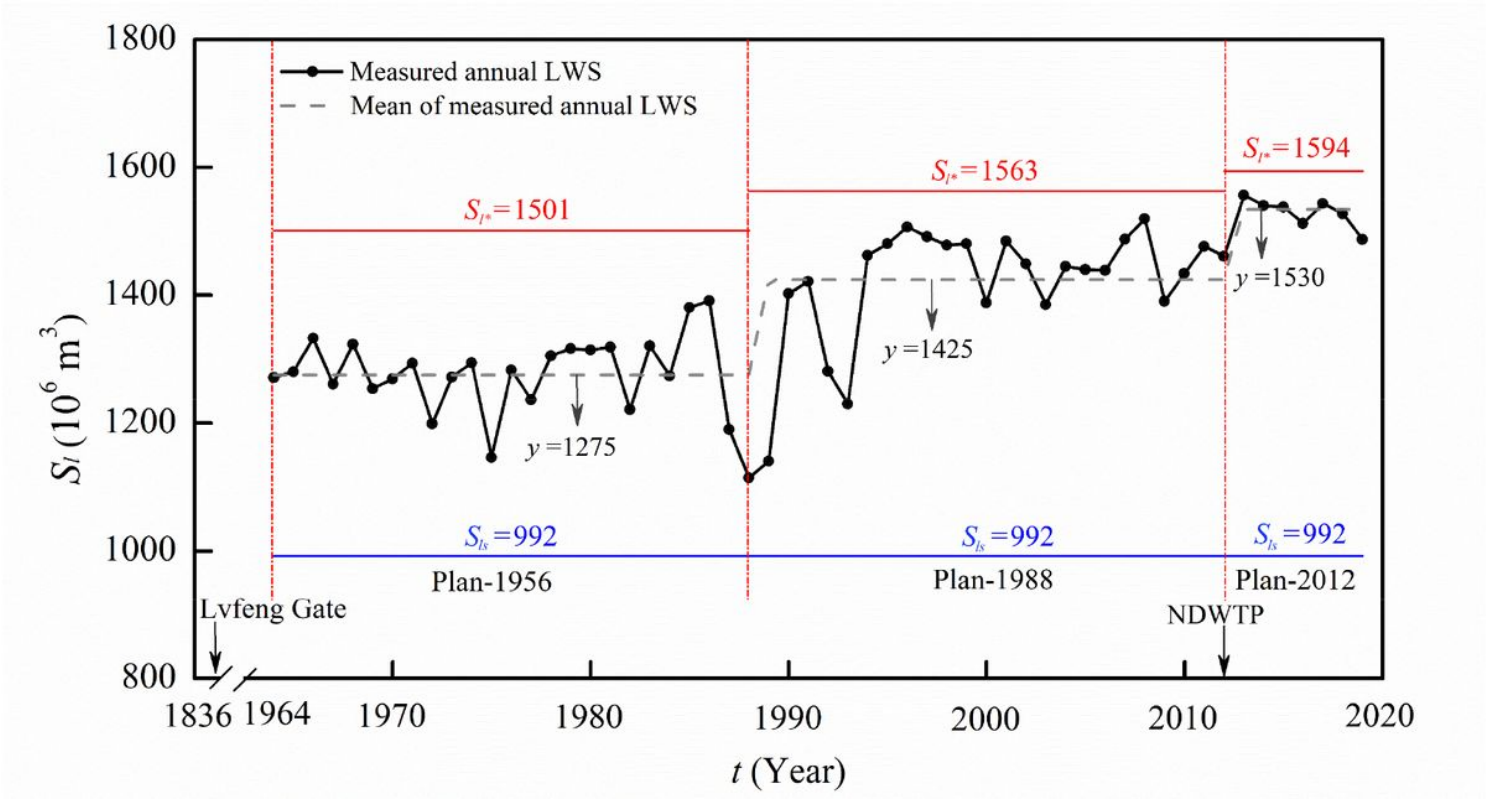

Figure 2

Variation of observed annual LWS under three different regulation plans in Lake Dianchi during 1964–2019

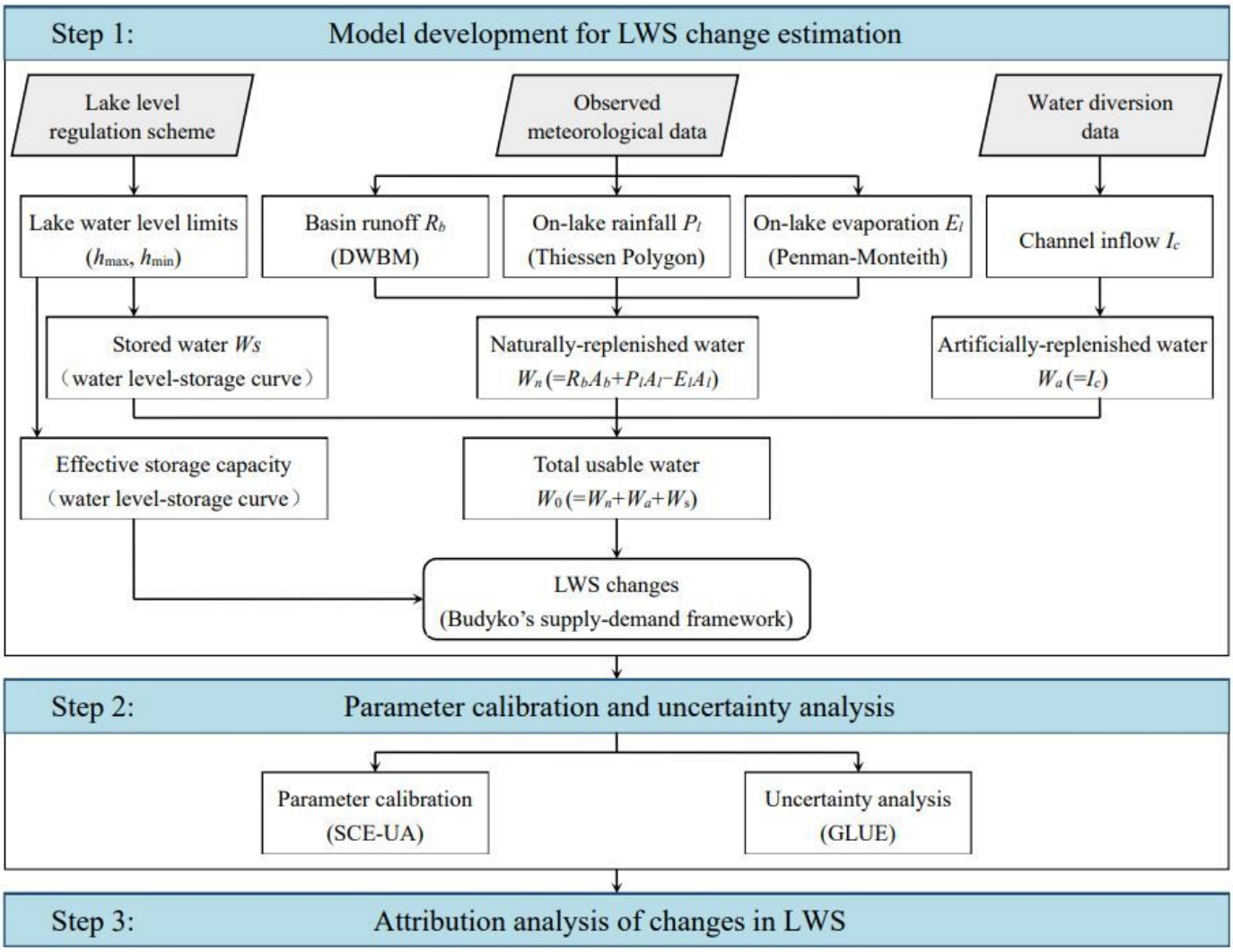

Figure 3

Flowchart for the estimation and attribution of water storage changes in regulated lakes, in which DWBM represents the dynamic water balance model developed by Zhang et al. (2008)

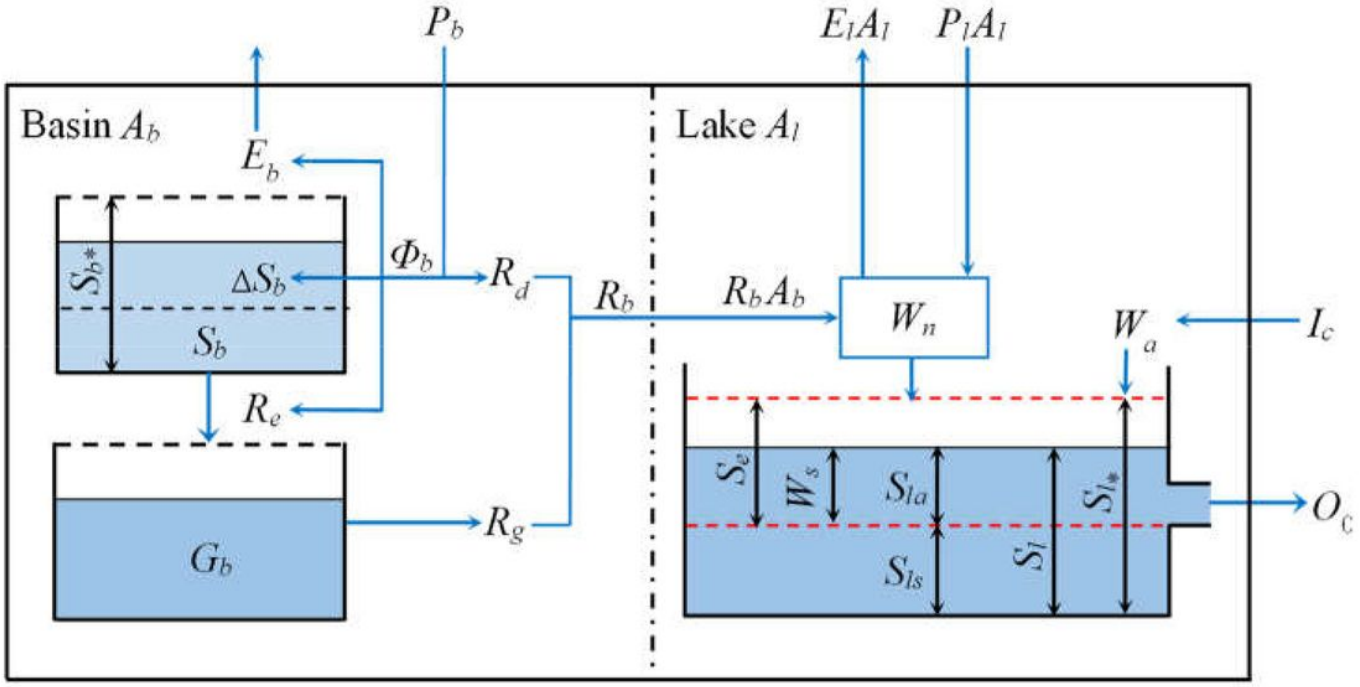

Figure 4

Schematic diagram of the main components in the Budyko-based LWS change estimation model

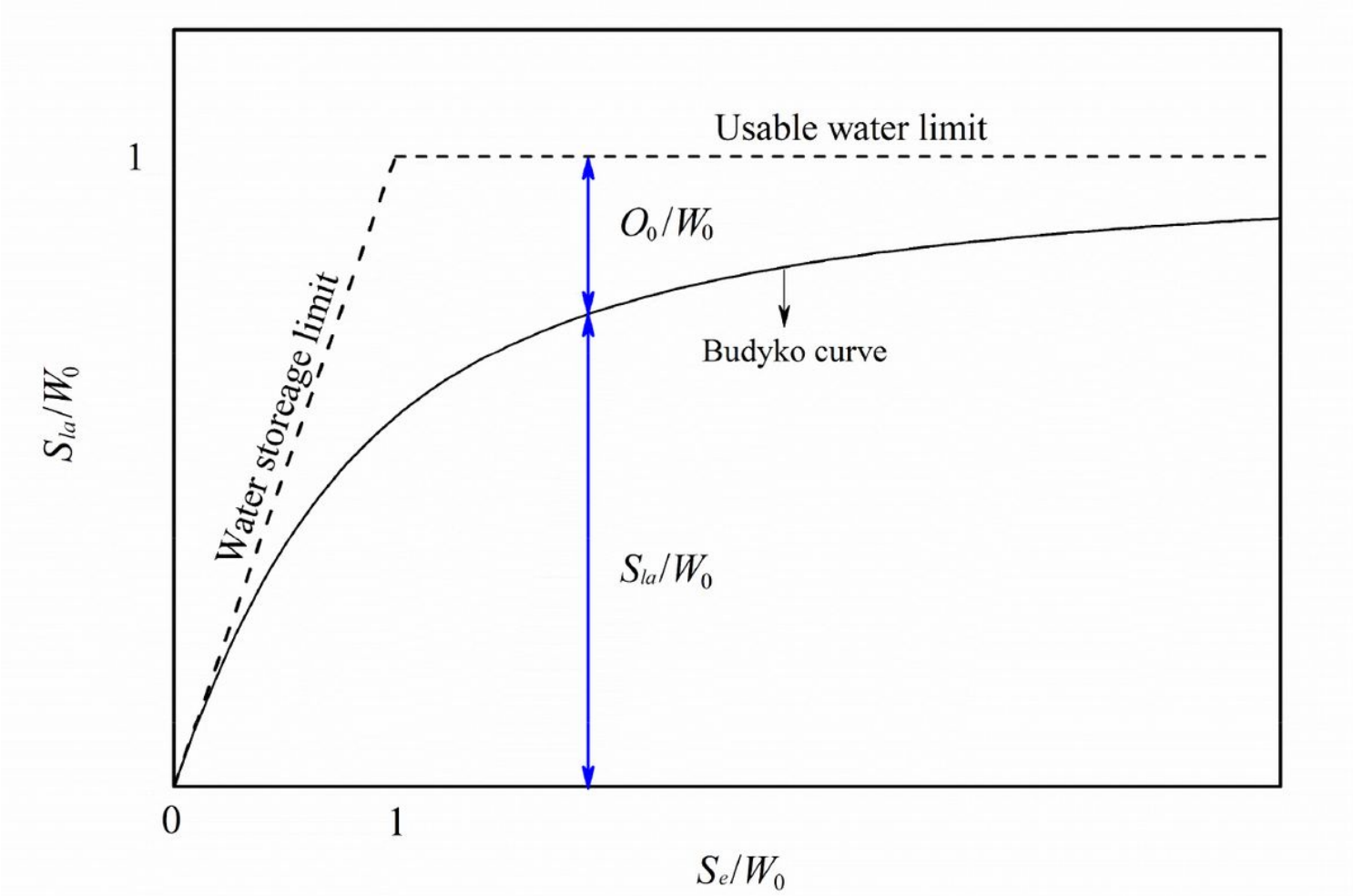

Figure 5

Budyko curve for active LWS in regulated lakes

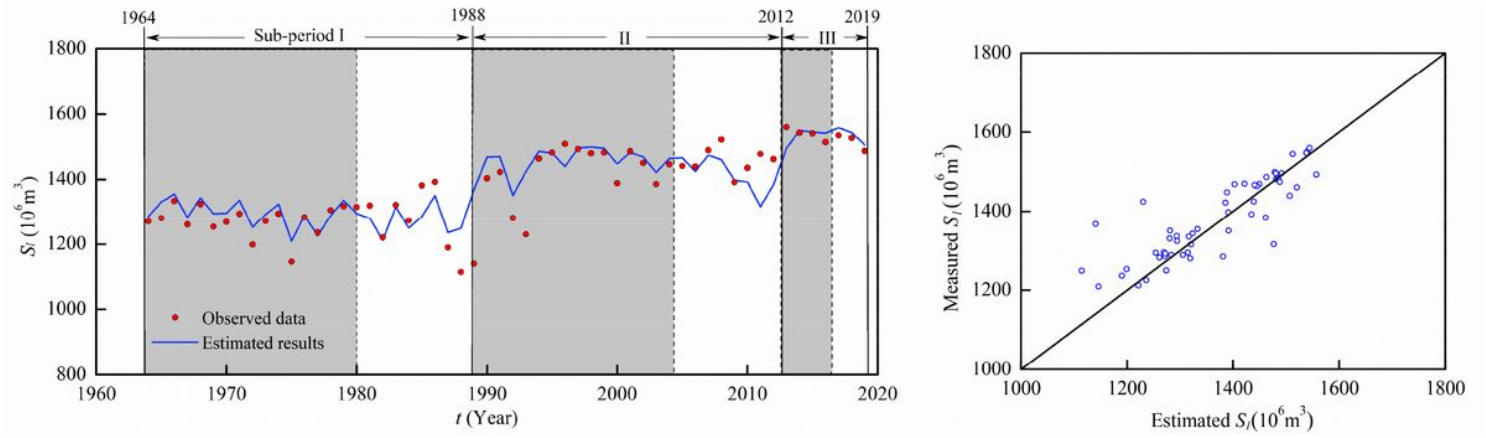

Figure 6

Comparison of estimated results with observed annual LWS in Lake Dianchi during 1964– 2019, in which the grey bands indicate the calibration periods, the white bands the validation periods

Figure 7

Budyko curves for LWS in Lake Dianchi

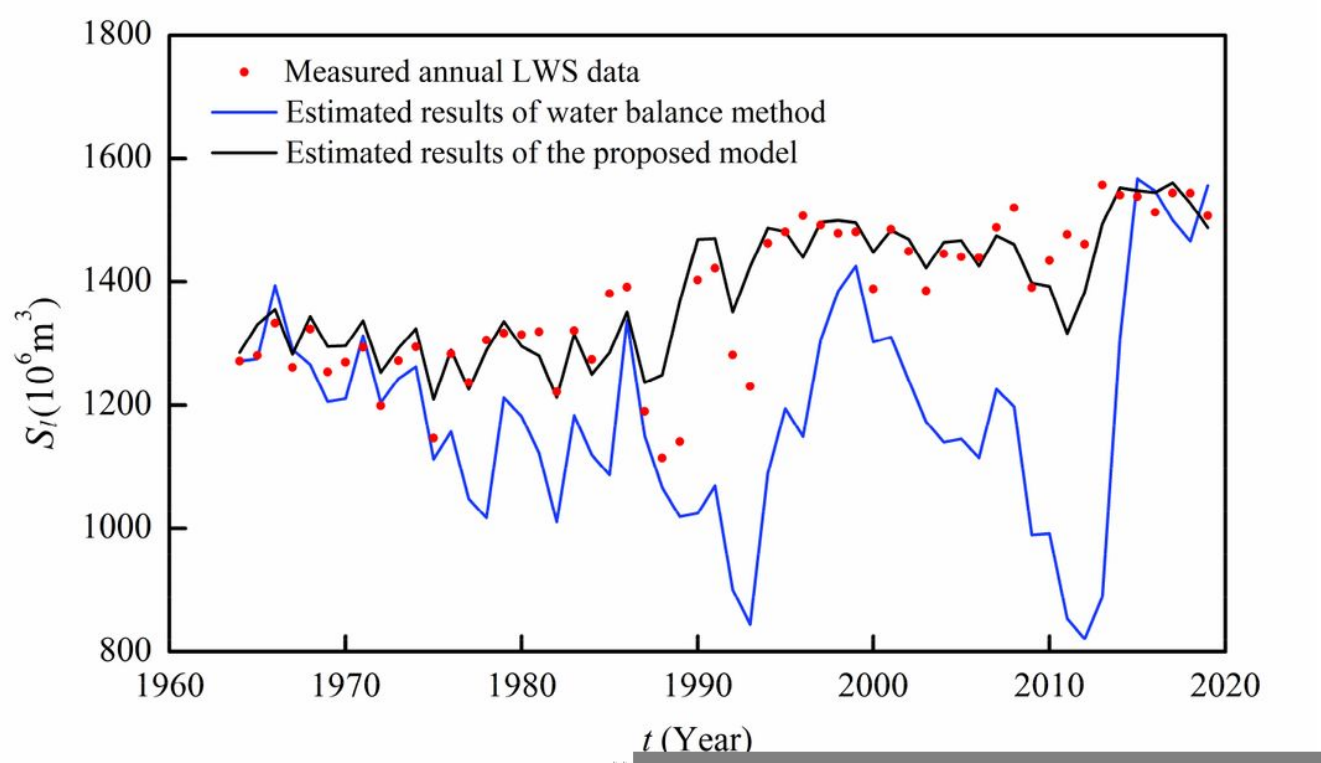

Figure 8

Comparisons of estimated annual LWS by the proposed model and HM-based water balance method with measured data in Lake Dianchi

Supplementary Files

This is a list of supplementary files associated with this preprint. Click to download.

- Highlights.docx